IEEE Robotics and Automation Letters (RAL) paper presented at the
2020 IEEE/RSJ International Conference on Intelligent Robots and Systems (IROS)
October 25-29, 2020, Las Vegas, NV, USA (Virtual)

ModMan: An Advanced Reconfigurable Manipulator System with Genderless Connector and Automatic Kinematic Modeling Algorithm

Alchan Yun[1,2], Deaho Moon[1], Junhyoung Ha[1], Sungchul Kang[3], and Woosub Lee[1,4,*]

***Abstract*— With the current trend of dwindling life cycle of production, necessity of systems with high-adaptability is on the rise. With their high adaptability and easy maintenance, reconfigurable manipulators are strong candidates to replace conventional non-reconfigurable manipulators in such trend. However, most of existing reconfigurable robots are designed for non-industrial use and remained in laboratory level because of their low accuracy and low mechanical/electrical capacity. In this paper, we present our newly developed manually reconfigurable manipulator, ModMan, equipped with genderless connectors which feature high mechanical/electrical capacity and multi-DOF modules, which are to increase the number of possible configurations while minimizing loss of manipulator performance. An automatic kinematic modeling algorithm for reconfigurable manipulators is also presented to deal with complexities due to genderless connections and multi-DOF modules. Evaluations of repeatability of 6-DOF configuration are performed to prove that the performance of ModMan is comparable to existing non-reconfigurable manipulators. Experiments on reconfiguration of kinematics for arbitrary connections of modules are also demonstrated.**

***Index Terms*— Reconfigurable Manipulator, Modular Robot, Genderless Connector, Kinematic Modeling.**

I. Introduction

Vastly escalating demands towards improved machinery based on individual needs, favoring principles of industry 4.0, promote higher level of adaptability. Conventional industrial manipulators with fixed configurations, referred to as *non-reconfigurable* throughout this paper, are usually deployed to meet such demands, which show satisfactory performance in general. However, their workspaces are limited to fixed volumes and they may not be optimal to certain tasks in terms of several performance measures such as time and power consumption. In addition, it takes much time to recover from hardware failures for non-reconfigurable manipulators because only experts can repair them. To overcome such weaknesses of non-reconfigurable manipulators, reconfigurable manipulators are introduced and investigated in literature to give users insight to configure their own optimal manipulator and to easily replace broken components for fast recovery from failures [1].

[1] A. Yun, D. Moon, J. Ha, and W. Lee are with the Center for Medical Robotics, KIST, Seoul 02792, South Korea (e-mail: {t16846, dmoon0322, jhha, robot}@kist.re.kr).

[2] A. Yun is with the Department of Mechanical and Aerospace Engineering, Robotics Laboratory, Seoul National University, Seoul 08826, South Korea (e-mail: comdam86@snu.ac.kr).

[3] Sungchul Kang is with Robot Center, Samsung Research, Seoul 06765, Korea (e-mail: kasch804@gmail.com).

[4] Woosub Lee is with Division of Nano & Information Technology, KIST School, UST, Daejeon 34113, Korea (e-mail: robot@kist.re.kr).

* Corresponding author: Woosub Lee.

The *modularity* is the degree to which a system's components can be separated and recombined so that the complexity of each part can be hidden and simply interfaced with others as described in [2]. In modular robot design, this paper defines modularity in terms of the concepts of *Degree of Reconfigurability (DOR), the number of possible combinations with the number of modules; and* Integrity*, the quality of integration.* Among manipulators with same kinematic structure, one is considered to have higher integrity if it has smaller number of parts with better performance measures. Thus, a non-reconfigurable robot is considered to have the highest integrity. Designing a well modularized manipulator system is equivalent to increasing both DOR and integrity, however, there is an inherent trade-off between DOR and integrity. Higher DOR is normally achieved by increasing the number of connection ports and the kinds of module, which degrades integrity simultaneously. In this paper, we propose that applying genderless connectors and multi-DOF modules compensates such weakness in a modular robot system. Genderless connectors increase DOR by two to the power of the number of modules. Multi-DOF joints improve integrity by reducing parts and space for connectors with the ease of downsizing [3].

Extensive surveys of the research literature on modular robots [4]–[7] show that the majority of such literature is on self-reconfigurable modular robots. Such robots have separate actuators for self-reconfiguring function to form desired configurations. However, the parts related to the function lower the integrity of the robots because they take up much space and weight. Hence, a manually reconfigurable modular manipulator with higher integrity would be preferable over a self-reconfigurable modular manipulator for industrial applications.

There have been several attempts to develop a manually reconfigurable modular robot manipulator suitable for industrial applications. Reconfigurable Modular Manipulator System (RMMS) [8], [9] is one of the earliest implementations of such a manipulator. Schunk has developed and commercialized LWA series [10], manually reconfigurable manipulators comprising 2 DOF modules, Powerball. Recently, Acutronic Robotics released Modular Articulated Robotic Arm (MARA) together with Hardware Robot Operating System(H-ROS) [11]. Though the robots are manually reconfigurable manipulators, they have a limited DOR due to their gendered connection.

A key design feature of a reconfigurable manipulator is the connector. In [12], a modular robot, Thor, is presented with a genderless connector based on spring-loaded pins for electri-

cal signals. In [13], a genderless connector with mechanical connection mechanism, HiGen, is presented. HiGen utilizes four hooks around a central axis for mechanical connection, and a circular spring-pin array for electrical connection. The mechanical and electrical connections of the genderless connectors, however, are not strong enough for industrial applications and are of low current capacity due to the small number of spring pins, respectively. In our previous works [14], [15], a genderless connector is presented with a robust mechanical design and an effective layout of spring pins. In this paper, we present an optimized genderless connector based on the previous works, whose performance is capable of industrial applications.

In line with advances in modular robot manipulator hardware design, there have been corresponding advances in modular robot manipulator software design, especially with respect to kinematics. In [16], a kinematic modeling of a modular robot manipulator by means of Denavit–Hartenberg (DH) parameter representation is proposed. This representation, however, is inadequate for modular robot manipulators because it needs to re-define each link frame when connections change. In [17], modern screw theoretic representations of kinematics of a modular robot manipulator is proposed. They defined the connections in terms of Assembly Incidence Matrix (AIM) and Accessibility Matrix (AM) to represent how the modules are connected and to describe the kinematics of their manipulator in a coordinate independent manner. In [18], a connector-graph representation for module assembly is defined to add an offset angle value at each connection. The aforementioned researches share a common limitation; each of their joint modules is of 1-DOF with a fixed input–output port. Thus, joint modules of multi-DOF and multiple connection ports need to be considered in kinematic modeling. In [3], Adaptive Robotic System Architecture (ARSA) is introduced to deal with more general types of modules and connections of modules by defining Object Incidence Matrix (OIM), which contains module-specific kinematic/dynamic parameters. Yet, no systematic kinematic modeling algorithm with such architecture is presented.

In this regard, the contribution of this work is to significantly improve the completeness of reconfigurable modular manipulator on both hardware and software sides. On the hardware side, the module designs are expanded and the connectors are further optimized from the ones in our previous works [14]. By having 2-DOF, the new joint modules achieve better integrity. Compared to the previous version of [14], the proposed genderless connector can withstand greater mechanical forces and transmit more electricity through pin layout optimization. On the software side, we introduce a novel automatic kinematic modeling algorithm that detects the kinematic structure and builds the kinematic model accordingly for any arbitrary tree structure. Connection-dependent parameters and module intrinsic parameters are carefully identified to efficiently build the kinematic model using the minimum amount of information transmitted through the connectors. As a complete system

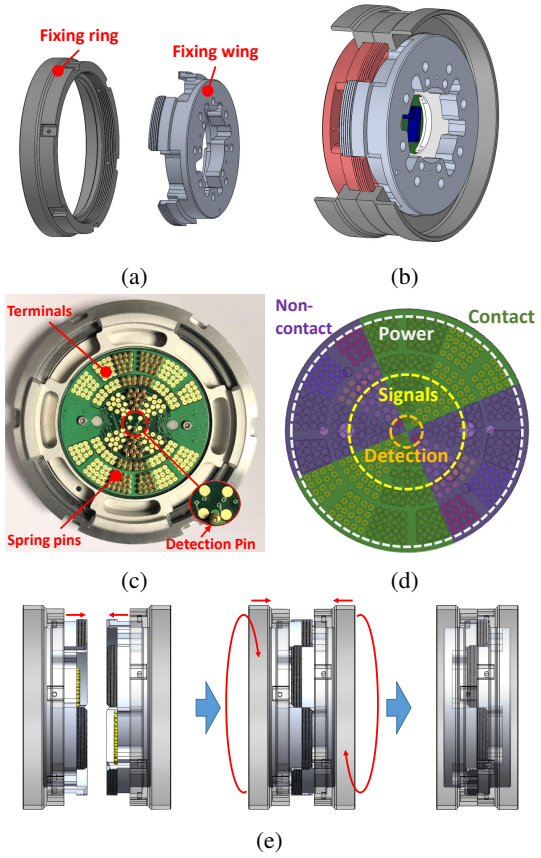

Fig. 1: Genderless Connector: (a) fixing ring and wing, (b) mechanical connection, (c) arrangement of spring pins and terminals, (d) electrical connection, (e) connection diagram.

to demonstrate the integration of the developed components, we built a modular manipulator system named *ModMan*.

This paper organized as follows. Section II describes the developed hardware, including genderless connector, joint, and link. Section III describes the automatic kinematic modeling algorithm for reconfiguration of a modular robot manipulator. Section IV shows experimental results regarding repeatability and reconfigurability of ModMan. Section V concludes the paper with further comments.

II. Hardware Development for Reconfigurable Robot Manipulator

In this section, the hardware components to build the modules of ModMan system are presented. A genderless connector, granted for US patent [19], is developed with enough mechanical/electrical capacity to withstand loads of 6 or 7-DOF manipulators. Details of joint unit, a collection of parts that corresponds to 1-DOF, are also presented. Based on those, 7 types of joint modules, 2 types of link modules, and a single type of gripper modules are built.

A. Genderless Connector

The genderless connector of ModMan consists of a mechanical connection mechanism and electrical connections as illustrated in Fig. 1. To give joint modules to have different

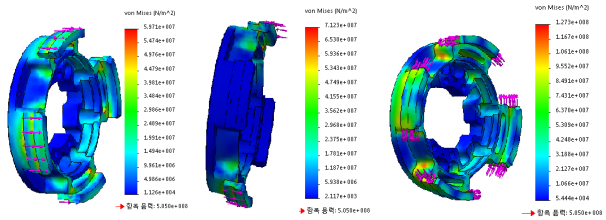

(a) (b) (c)

Fig. 2: FEM Result: (a) tensile force of 1000N, (b) torsion about radial direction of 160Nm, (c) torsion about axial direction of 160Nm.

range of motion, the connector is designed to be connectable in every 90° angle for 4 different offset angles.

For an intuitive and solid connection, a simple screw fastener with extruded features was adopted for mechanical connection mechanism as shown in Fig. 1a. The fastener consists of fixing rings with inner threads and fixing wings with outer threads. As illustrated in Fig. 1e, each fixing wing is fastened with the fixing ring of the other side. The fastened structure of Fig. 1b can support bending and torsional stresses in all directions. Note that the mechanical connection between two fixing wings is of a sliding fit to minimize error and backlash at the connection. Although it is possible to tighten the fastener by hand, it is best to use a hook spanner to ensure a promising connection.

To guarantee the structural safety of ModMan, the finite element method (FEM) was applied on SolidWorks to analyze the fixing wing's stiffness and the results are shown in Fig. 2. An extremely high tensile force of 1,000 N was applied to the fixing wing and the resulting maximum stress was $5.97\times10^7 N/m^2$ which has an associated factor of safety (FoS) of 8.46. A torsion of $160Nm$ — the maximum peak torque of the large joint module (Table 2) — was applied to the fixing wing and the resulting maximum stresses about the radial and axial directions are $7.12 \times 10^7 N/m^2$ and $1.27 \times 10^8 N/m^2$ which have associated FoS of 7.09 and 4.97, respectively. Because these results are for a single fixing wing only, the actual FoS of the assembly by two fixing wings and rings are to be doubled at least. All of the results ensure that the geometric structure of the mechanical connection is more than safe in all directions. Note that our previous version of [14] has FoS of 2.81 and 2.70 for same tensile force and torsion about the radial direction, respectively, and the maximum stress for the torsion about axial direction exceeds the yield strength of the structure. The results imply that the structural strength of the proposed version is superior to the previous one.

The electrical connections of the genderless connector (Fig. 1c) are responsible for transferring electrical power and communication signals between the modules. Contacts between spring pins and surface terminals are used for the connection to give compliance for robustness against mechanical clearances. As illustrated in Fig. 1d, the electrical connection is divided into three sections: inner section for

System	Type	Power	Signals	Number of Spring Pins
RMMS [8]	Gendered	72V-25A 48V-6A	2 RS-485, 4 Videos	30
Powerball [10]	Gendered	24V-15A	CANopen, 10 Signals	20
MARA [11]	Gendered	48V-8A	Ethernet	16
Thor [12]	Genderless	2 Pins	RS-485,	6
HiGen [13]	Genderless	4 Pins	I2C, Serial	12
ModMan [14] (previous)	Genderless	20 Pins	EtherCAT, 18 Signals	46
ModMan (proposed)	Genderless	88 Pins (48V-56A 5V-48A)	EtherCAT, 22 Signals	115

TABLE 1: An electrical capacity comparison of connectors in reconfigurable modular robot systems.

Model	Large	Medium	Small
Weight	5.36 Kg	4.45 Kg	3.7 Kg
Motor	TBMS-7615A	TBMS-6013A	RBE-01211A
Gear ratio	1 : 100	1 : 100	1 : 100
Rated torque	93.9 Nm	41.5 Nm	22.3 Nm
Peak Torque	157 Nm	82 Nm	54 Nm
Speed	42.26 rpm	54.2 rpm	103.47 rpm
Encoder	19 bit	19 bit	19 bit
Resolution	0.002 deg	0.002 deg	0.002 deg

TABLE 2: Specification of 2-DOF joint modules.

a detection pin to recognize offset angle, middle section for 26 signals including Ethernet for Control Automation Technology (EtherCAT) signals, and outer section for power and ground. To enable the connection at every 90° and maximize the number of the contacts, the spring pins are arranged in two diametrically opposite octants. Note that the detection pin is located in only one of the octants for 90° resolution. Two sets of the surface terminals are arranged in mirrored pattern of the arrangement and placed with $\pm45^\circ$ angles. Based on the effectively designed layout, a total of 115 spring pins are mounted on the connector. With this numerous number of spring pins, the ModMan genderless connector can transfer greater amounts of power and signals than the other connectors as shown in Table 1. The performance of the ModMan genderless connector is able to support loads of high-DOF configurations such as a dual-arm configuration.

B. Joint Modules

The joint units of different sizes (small, medium, and large) but of a common structure were developed for ModMan and an example of the large joint unit is shown in Fig. 3. The structure of the joint units shares some of the features with the actuation unit introduced in [20]. The design of the joint unit mainly focuses on optimal spacing. Both joint side and link side displacements are delivered to the opposite side of output flange by couplings and are measured using two absolute encoders. The genderless connector is to be attached on the output flange and a motor brake is placed behind the

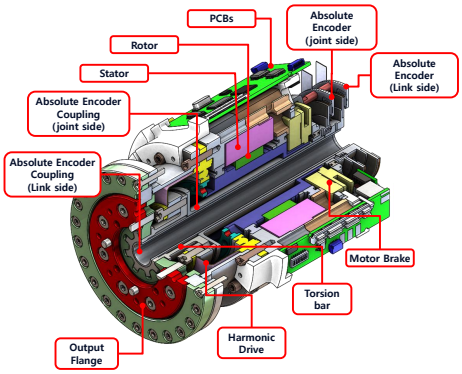

Fig. 3: Details of the joint unit of large size.

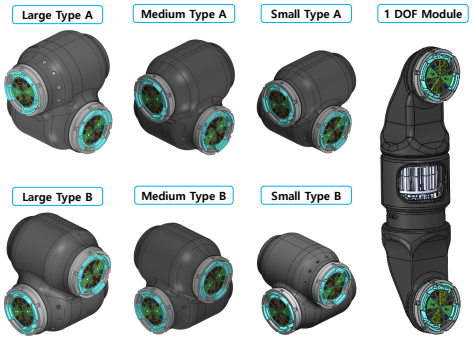

Fig. 4: 2-DOF joint modules and 1-DOF joint module.

motor for the safety reason. Details of the specifications of each of the joint unit are described in Table 2.

For effective management and development of the modules, three types of PCBs are developed in a modular manner; controller PCBs for computations, EtherCAT PCBs for communication, and motor driver PCBs for amplification of motor inputs. Since EtherCAT communication protocol has a directional property of data in/out ports, a switching circuit is implemented to change the direction of EtherCAT communication. All the types are designed to have the same geometry and can be connected to each other by flex cables so that a set of PCBs can wrap around a joint in a manner of minimizing the required space for installing them.

To configure various types of manipulators, several types of joint modules were developed as shown in Figure 4. To build a 2-DOF module, two joint units of same size can be assembled in infinitely many ways but we chose two ways of assembling them in orthogonal directions with offset, which we label “type A” and “type B”. In total, there are six 2-DOF modules built which consist of two different types with three different sizes. By using all six 2-DOF modules, we can build two typical manipulators - ”left” and ”right” arms - which will be shown later.

In addition to the 2-DOF joint modules, a 1-DOF joint module, which is shown in Fig. 4, was developed whose joint unit is identical to that of the 2-DOF joint module of large size. It is assembled following the first 2-DOF joint module to configure a typical 7-DOF manipulator.

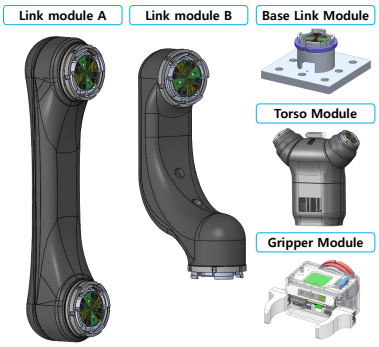

Fig. 5: Link and gripper modules.

C. Link and Gripper Modules

In addition to the joint modules, four link modules - each featuring genderless connectors - are also developed to configure various types of manipulators as shown in Fig. 5. ”Link module A” and “Link module B” are designed for upper and lower arms, respectively. Likewise, ”Base link module” and “Torso” are designed for one-arm and human-like dual arm configurations, respectively. Note that link modules also act like a slave even though they do not have any actuators because their directions and angles of connections need to be automatically detected and considered for kinematic reconfiguration. Thus, each link module has a controller and an EtherCAT PCBs. The weights of link module A and B are $3.88Kg$ and $3.4Kg$, respectively.

For the proof of concept, we also designed a gripper module as shown in Fig. 5. The gripper has a driver PCB for actuation in addition to the low-level controller and EtherCAT PCBs. The jaws of the gripper module are coupled to each other to be driven by a single actuator. It has a function to detect gripping force using spring deflection to pick soft objects. The gripper also utilizes a RGB-D sensor (RealSense SR300) to perform simple vision based pick-and-place tasks.

III. Automatic Modeling of the Manipulator Kinematics

Because the ModMan system is based on genderless connectors and multi-DOF joint modules, kinematic modeling of ModMan requires extra considerations on how the modules can be broken down into joint/link elements. For example, a 2-DOF joint module of minimum number of connectors consists of three link elements, two joint elements, and two connection ports as illustrated in Fig. 6. In light of such considerations, we developed an automatic kinematic modeling algorithm for use with tree-structured reconfigurable manipulators and it is applied to ModMan.

A. Kinematic Modeling

In what follows, we use the modern screw-theoretic formulation of kinematics as outlined in [21], [22]. The task space of a robot can be defined on the space of the special Euclidean group $SE(3)$ while the 4×4 rigid body

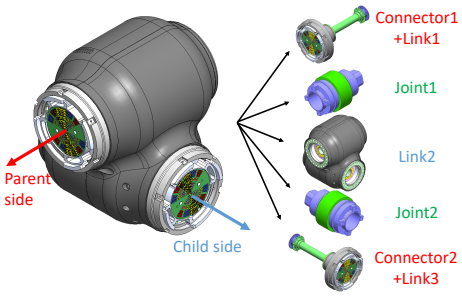

Fig. 6: Hierarchy of 2-DOF module.

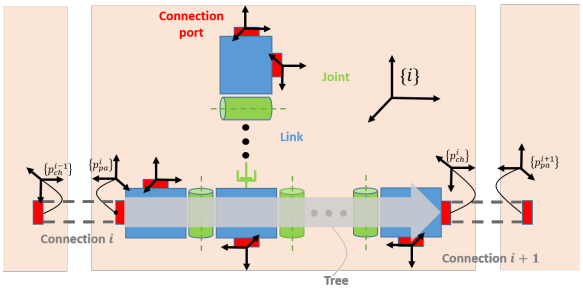

Fig. 7: Illustration of generalized module.

transformation matrix $T \in SE(3)$ is of the form

$$T = \begin{pmatrix} R & x \\ 0_{1\times 3} & 1 \end{pmatrix}, \tag{1}$$

where R is the 3 by 3 rotation matrix, $x \in \mathbb{R}^3$ is the position vector. For any $T \in SE(3)$, one can find corresponding screw parameter $A \in \mathbb{R}^6 = \left(\omega^T, v^T\right)^T$ with $\omega, v \in \mathbb{R}^3$, which satisfies the matrix exponential of the form

$$T = e^{[A]}. \tag{2}$$

The square bracket notation $[A]$ for screw parameter A denotes

$$[A] = \begin{pmatrix} [\omega] & v \\ 0_{1\times 3} & 0 \end{pmatrix}, \tag{3}$$

where, again, the square bracket notation $[\omega]$ for three dimensional vector $\omega = (\omega_1, \omega_2, \omega_3)^T$ is

$$[\omega] = \begin{pmatrix} 0 & -\omega_3 & \omega_2 \\ \omega_3 & 0 & -\omega_1 \\ -\omega_2 & \omega_1 & 0 \end{pmatrix}. \tag{4}$$

To find a systematic way of kinematic modeling of an assembled reconfigurable manipulator of tree structure, we first defined a *generalized module* as illustrated in Fig. 7. Assuming it is i'th module in the corresponding branch, the generalized module itself is a tree structure which consists of P^i number of connection ports - each of which can be connected to a parent-side or to a child-side - and K^i joint elements with screw parameters $A^i_J \in \mathbb{R}^6, J = 1, \cdots, K^i$, are described in module frame $\{i\}$. The joint elements are assumed to be either revolute or prismatic joint. Although joint elements of higher DOF than one can be treated in a manner similar to that of one DOF as described in [23], they are not considered here because of their rarity in industrial manipulators.

A generalized module i can have $S^i = P^i(P^i - 1)$ possible permutations for one serial connection. When a serial connection is made, unique branch can be retrieved and it is represented as a collection of indices of the form $B^i_s = \{pa_s, J_{s,1}, \cdots, J_{s,k^i}, ch_s\}, s = 1, \cdots, S^i$, where pa_s is the index of parent-side connection port, ch_s is the index of child-side connection port, and $J_{s,j}, j = 1, \cdots, k^i$ are the indices of the corresponding joint elements with k^i number of the effective joint elements of the branch. Once connected, unique branch index s can be found with k^i effective joint elements and $k^i + 1$ link components.

Let us assume m modules are serially connected to construct an n DOF manipulator and each module has its own module frame $\{i\}, i = 1, \cdots, m$. The forward kinematics $T_{0,e}$, which is the transformation from base frame $\{0\}$ to end-effector frame $\{e\}$, can be expressed as

$$T_{0,e} = T_{0,p^1_{pa}} T_{p^1_{pa},p^2_{pa}} \cdots T_{p^{m-1}_{pa},p^m_{pa}} T_{p^m_{pa},e} \tag{5}$$

where $T_{p^i_{pa},p^{i+1}_{pa}} \in SE(3)$ is a *modular kinematics* of module i which is the transformation matrix from parent port frame of module i, $\{p^i_{pa}\}$, to parent port frame of module $i+1$, $\{p^{i+1}_{pa}\}$. $T_{p^m_{pa},e} \in SE(3)$ is the transformation matrix defined at end-effector module. Assuming all link frames are initially coincide with the module frame $\{i\}$, $T_{i,l}$, the transformation from module frame $\{i\}$ to link element frame $\{l\}, l = 0, \cdots, k_i$, can be described as

$$T_{i,l} = \begin{cases} I_{4\times 4} & \text{if } l = 0 \\ e^{[A^i_{J_{s,1}}]\theta_{\psi+1}} \cdots e^{[A^i_{J_{s,l}}]\theta_{\psi+l}} & \text{otherwise,} \end{cases} \tag{6}$$

where $\psi = \sum_{q=1}^{i-1} k_q$. Now the modular kinematics of module i can be described as

$$\begin{aligned} T_{p^i_{pa},p^{i+1}_{pa}} =& M^{-1}_{i,p^i_{pa}} e^{[A^i_{J_{s,1}}]\theta_{\psi+1}} \cdots e^{[A^i_{J_{s,k_i}}]\theta_{\psi+k_i}} \\ & \cdot M_{i,p^i_{ch}} T_{p^i_{ch},p^{i+1}_{pa}} \end{aligned} \tag{7}$$

where $M_{i,p^i_{pa}}, M_{i,p^i_{ch}} \in SE(3)$ are initial transformations from module frame $\{i\}$ to parent port frame $\{p^i_{pa}\}$, child port frame $\{p^i_{ch}\}$, respectively, $T_{p^i_{ch},p^{i+1}_{pa}}$ is the transformation from i-th child port frame $\{p^i_{ch}\}$ to $i+1$-th parent port frame $\{p^{i+1}_{pa}\}$, of which the value is dependent on offset angle ϕ_i between module i and module $i+1$. For systematic derivation of $T_{p^i_{ch},p^{i+1}_{pa}}$, we assume there are distinct reference frames at every connection port and the orientation of the frame is defined in a consistent manner; in this paper we choose the outward normal direction at a connection port to be $\hat{z}$-direction and the direction of the reference line for the offset angle to be $\hat{x}$-direction. Now $T_{p^i_{ch},p^{i+1}_{pa}}$ can be defined as

$$T_{p^i_{ch},p^{i+1}_{pa}}(\phi_i) = \begin{pmatrix} \cos\phi_i & \sin\phi_i & 0 & 0 \\ \sin\phi_i & -\cos\phi_i & 0 & 0 \\ 0 & 0 & -1 & 0 \\ 0 & 0 & 0 & 1 \end{pmatrix}. \tag{8}$$

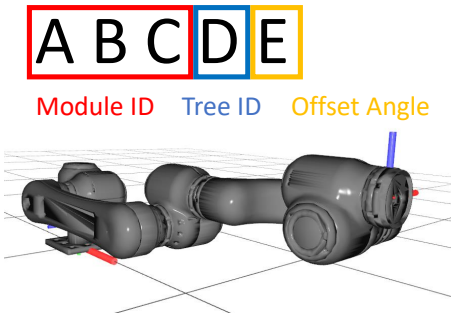

Fig. 8: Connection protocol and configured manipulator in its zero position with 00010 - 21114 – 00212 – 22214 – 00512 – 23112 – 00101 (base-LargeA-LinkA-MedB-LinkB-SmallA-Dummy).

An advantage of the screw-theoretic kinematics is that the manipulator Jacobian is efficiently computed by transforming the reference coordinate of screw parameters of each joint to end-effector frame [21].

B. Model Parameter Classification

The model parameters described above need to be partitioned into two groups; module intrinsic parameters and connection-dependent parameters. The module intrinsic parameters, whose values should be provided prior to connection, are

- $M_{i,p_q^i} \in SE(3), q = 1, \cdots, P^i$, initial transformation matrices from module frame $\{i\}$ to connection port frames p_q^i,
- $A_J^i \in \mathbb{R}^6, J = 1, \cdots, K^i$, screw parameters of joint elements described in module module frame $\{i\}$,
- $B_s^i = \{pa_s^i, J_{s,1}^i, \cdots, J_{s,k^i}^i, ch_s^i\}, s = 1, \cdots, S^i$, all possible branches in form of a series of indices for corresponding parent port, joint elements and child port.

The connection-dependent parameters, whose values are determined upon connections, are

- t, the module ID,
- s, the index of kinematic tree,
- ϕ, offset angle of connection,

Note that as the number of possible permutation S^i increases proportional to square of the number of connection ports P^i, it is arguable to consider B_s^i as an intrinsic parameters. Modules with small number of ports, such as those of ModMan, will have small value of S^i. Thus, it is efficient to have the values of B_s^i for every branches prior to connections and to recognize the branch ID s upon connection. For the modules with many connection ports, the module itself should be capable of automatically retrieving the branch B_s^i when a connection is made.

In this research, the connection-dependent parameters follow a protocol, 5 digit integer, as shown in Fig. 8. First 3 digits represent the module ID, forth and fifth digits represent tree ID and offset angle, respectively. Now the connection status of a configured manipulator can be represented as a series of integers. An example of 6-DOF right-arm configuration is illustrated in Fig. 8.

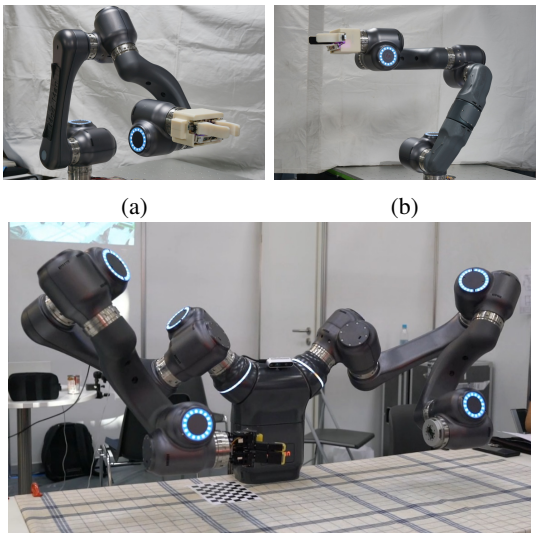

(a) (b)

(c)

Fig. 9: Examples of different configurations: (a) 6-DOF, (b) 7-DOF, (c) dual arms.

Examples of possible configurations with developed modules are shown in Fig. 9. Since every modules can be represented as a generalized module, proposed algorithm supports not only joint + link connections but also link + link or joint + joint connections such as connecting 2-DOF large module + 1 DOF module appeared in 7-DOF manipulator.

The kinematic model obtained through the above process can be used to perform the actions defined in the task space and characterize the robot's workspace. Because of the nature of the reconfigurable robots, the methods for the inverse kinematics and the workspace characterization should be applicable to general kinematic structures; examples are the Newton-Raphson numerical inverse kinematics described in [21] and the workspace boundary determination described in [24], respectively.

IV. Experiments

We performed two different hardware experiments. An accuracy evaluation is performed to prove that the repeatability of a 6-DOF configuration of ModMan system is comparable that of non-reconfigurable manipulators. We also conducted a reconfiguration test to see the validity of the automatic kinematic modeling algorithm presented in previous section.

A. System Setup

To validate the performance of ModMan compared to conventional manipulators, we developed software for low-level controls and high-level commands.

For the independent joint control, a discrete PID controller for position control is implemented. The output is link-side angle and the motor input is pulse width modulation (PWM). A discrete-time first-order low-pass filter, also known as an

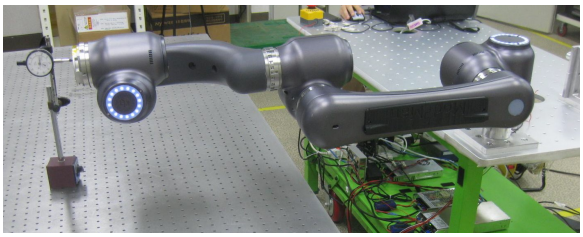

Fig. 10: Environment for repeatability test.

Trial	Displacements(mm)	Trial	Displacements(mm)
1	0.2	11	0.22
2	0.18	12	0.23
3	0.17	13	0.22
4	0.20	14	0.20
5	0.19	15	0.20
6	0.21	16	0.18
7	0.22	17	0.21
8	0.22	18	0.19
9	0.20	19	0.17
10	0.21	20	0.19
Stand. Div.	**0.0169**	Max Diff	**0.06**

TABLE 3: Repeatability test results.

exponentially weighted moving average, is involved in the derivative term, and saturation is applied in the integral term.

To show that the automatic kinematic modeling algorithm works on actual hardware, we also built a software to visualize the ModMan system. When all the modules are connected, every slave sends their connection-dependent parameters to the master controller, which are forwarded to the visualization software. The kinematics of the manipulator is constructed using the algorithm of Section III and the simulation model is synchronized with the hardware using joint encoder values which is received every 10ms through TCP/IP communication. 3D mesh models of a module are separated into each link element as illustrated in Fig. 6 and all link coordinates are computed using Eq. (6).

B. Repeatability Comparison with Non-reconfigurable Robot Manipulators

To evaluate repeatability, the left 6-DOF configuration manipulator repeated a motion between two postures based on the trajectory planned by trapezoidal joint space planner. The values of the calibrated dial gauge were recorded when the robot hit the gauge tip with the second posture as illustrated in Fig. 10. The result is shown in Table 3. The maximum difference among values are $0.06mm$ with standard deviation of $0.0169mm$. One of the most widely used non-reconfigurable manipulators, UR5 of Universal Robot, has $\pm 0.1mm$ repeatability [25]. The result proves that our manipulator system is indeed comparable to existing non-reconfigurable manipulators in terms of repeatability. Note that the ModMan system only relies on the independent joint control. It implies that we still have capacity to improve its repeatability for more precise applications.

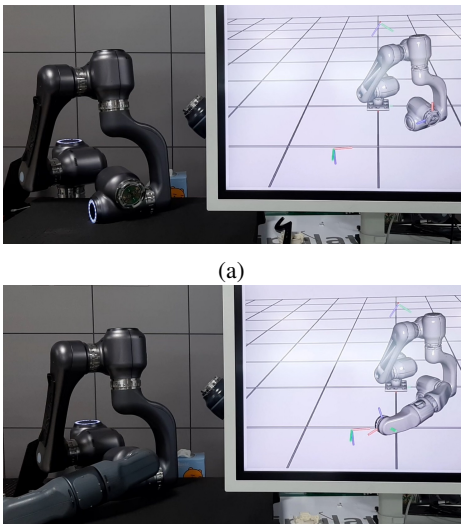

(a)

(b)

Fig. 11: Automatic kinematic modeling test: (a) 6-DOF, (b) 7-DOF.

C. Reconfigurability

Two different combinations of modules are tested for kinematic modeling and the results are shown in Fig. 11. The first configuration is a 6-DOF right-arm manipulator, which resembles properties of conventional 6-DOF non-configurable manipulators. The second configuration is formed by connecting a 1-DOF module at the end of the first configuration. The automatic kinematic modeling algorithm constructs the kinematics of the two manipulators successfully; the models are identical to the actual hardware postures.

To see if the manipulator Jacobian is properly found, we also conducted an experiment to follow task space trajectories. As described in Section III-A, manipulator Jacobian for differential kinematics can easily be obtained by transforming the reference coordinate of screw parameters of each joint to end-effector frame. Cartesian space planner is implemented using the numerical inverse kinematics and B-spline interpolation. A 7-DOF right-arm configuration is subjected to a task space trajectory whose orientation is constant and the result is illustrated in Fig. 12. The inverse of 6 by 7 Jacobian matrix is calculated with Moore-Penrose pseudo inverse for minimum norm solution. The end-effector successfully keeps its orientation constant during the motion.

V. Conclusion

In this paper, we present a reconfigurable manipulator system, ModMan, from hardware to software. The genderless connector shows high mechanical/electrical capacities capable of driving reconfigurable manipulators with up to 7 joint elements. The ModMan system has 7 joint modules and 4 link modules which can be assembled to configure various types of manipulators including widely used 6-DOF and 7-DOF manipulators. An automatic kinematic modeling algorithm for reconfigurable robot manipulators with a concept of generalized modules is proposed to deal with genderless

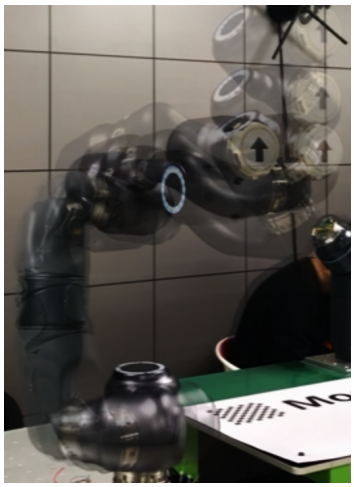

Fig. 12: Chronograph of Cartesian motion 7-DOF configuration. The end-effector orientation is visualized with an upward pointing arrow.

connections and multi DOF modules. Experimental results demonstrate that the repeatability of ModMan is comparable to that of conventional industrial non-reconfigurable manipulators. The reconfigurability of ModMan has also been validated on the real hardware with multiple arbitrary combinations of the modules.

By expanding the kinds of ModMan hardware modules, a user will be able to configure various other types of robot manipulator such as a Selective Compliance Assembly Robot Arm (SCARA) robot or a spherical robot. Simultaneously, the automatic kinematic modeling algorithm can be applied to any other reconfigurable robot systems. The automatic dynamic modeling algorithm, which will appear in our future work, allows us to come up with more sophisticated torque control algorithms and allows the ModMan to be reactive to external forces for safety so it can be considered as a cooperative robot.

ACKNOWLEDGMENT

This research was supported by the MOTIE (The Ministry of Trade, Industry and Energy), Korea, under the Robot industry fusion core technology development project(10048920) supervised by the KEIT(Korea Evaluation of Industrial Technology).

REFERENCES

[1] K. Stoy, D. Brandt, and D. Christensen, "Self-reconfigurable robots: An introduction,"The MIT Press, 2010.

[2] M. A. Schilling, "Toward a general modular systems theory and its application to interfirm product modularity," *Acad. Manage. Rev.*, vol. 25, no. 2, pp. 312–334, 2000.

[3] Z. Bi, Y. Lin, and W. Zhang, "The general architecture of adaptive robotic systems for manufacturing applications," *Robot. and Comput.-Integr. Manuf.*, vol. 26, no. 5, pp. 461–470, 2010.

[4] M. Satoshi and K. Haruhisa, "Self-organizing robots," in *Springer Tracts Adv. Robot.*, 2012.

[5] H. Ahmadzadeh, E. Masehian, and M. Asadpour, "Modular robotic systems: characteristics and applications," *J. Intell. & Robot. Syst.*, vol. 81, no. 3-4, pp. 317–357, 2016.

[6] M. Yim, W.-M. Shen, B. Salemi, D. Rus, M. Moll, H. Lipson, E. Klavins, and G. S. Chirikjian, "Modular self-reconfigurable robot systems [grand challenges of robotics]," *IEEE Robot. & Automat. Mag.*, vol. 14, no. 1, pp. 43–52, 2007.

[7] A. Brunete, A. Ranganath, S. Segovia, J. P. de Frutos, M. Hernando, and E. Gambao, "Current trends in reconfigurable modular robots design," *Int. J. Adv. Robot. Syst.*, vol. 14, no. 3, pp. 1–21, 2017.

[8] C. Paredis and P. Khosla, "RMMS: Reconfigurable modular manipulator system project," in *Video Proc. IEEE Int. Conf. Robot. Automat.*, January 1997, pp. 20–25.

[9] C. J. Paredis, H. B. Brown, and P. K. Khosla, "A rapidly deployable manipulator system," *Robot. Auton. Syst.*, vol. 21, no. 3, pp. 289–304, 1997.

[10] Schunk Gmbh & Co. KG., "Dextrous lightweight arm LWA 4D," 2010. [Online]. Available: https://schunk.com/fileadmin/pim/docs/IM0012315.PDF,

[11] N. G. Lopez, Y. L. .E. Nuin, E. B. Moral, L. U. S. Juan, A. S. Rueda, V. M. Vilches, R. Risto, "gym-gazebo2, A toolkit for reinforcement learning using ROS 2 and Gazebo," in *arXiv preprint arXiv:1903.06278*, 2019.

[12] A. Lyder, R. F. M. Garcia, and K. Stoy, "Genderless connection mechanism for modular robots introducing torque transmission between modules," in *Proc. ICRA Workshop Modular Robots, State of the Art*, 2010, pp. 77–81.

[13] C. Parrott, T. J. Dodd, and R. Groß, "HiGen: A high-speed genderless mechanical connection mechanism with single-sided disconnect for self-reconfigurable modular robots," in *IEEE/RSJ Int. Conf. Intell. Robot. Syst.,* IEEE, 2014, pp. 3926–3932.

[14] S. Hong, W. Lee, K. Kim, H. Lee, and S. Kang, "Connection mechanism capable of genderless coupling for modular manipulator system," in *2017 14th Int. Conf. Ubiquitous Robot. Ambient Intell.*, June 2017, pp. 185–189.

[15] S. Hong, D. Choi, S. Kang, H. Lee, and W. Lee, "Design of manually reconfigurable modular manipulator with three revolute joints and links," in *2016 IEEE Int. Conf. Robot. Automat.*, May 2016, pp. 5210–5215.

[16] L. Kelmar and P. K. Khosla, "Automatic generation of kinematics for a reconfigurable modular manipulator system," in *Proc. IEEE Int. Conf. Robot. Automat.,* IEEE, 1988, pp. 663–668.

[17] I-M. Chen and G. Yang, "Automatic generation of dynamics for modular robots with hybrid geometry," in *Proc., IEEE Int. Conf. Robot. Automat.*, vol. 3. IEEE, 1997, pp. 2288–2293.

[18] F. Hou and W.-M. Shen, "On the complexity of optimal reconfiguration planning for modular reconfigurable robots," in *2010 IEEE Int. Conf. Robot. Automat.,* IEEE, 2010, pp. 2791–2796.

[19] W. Lee, S. Hong, S. Kang, and K. Kim, "Module connection mechanism capable of genderless coupling," Dec 2017, US Patent 9853386B1.

[20] N. G. Tsagarakis, D. G. Caldwell, F. Negrello, W. Choi, L. Baccelliere, V.-G. Loc, J. Noorden, L. Muratore, A. Margan, A. Cardellino *et al.*, "Walk-man: A high-performance humanoid platform for realistic environments," *J. Field Robot.*, vol. 34, no. 7, pp. 1225–1259, 2017.

[21] K. Lynch and F. C. Park, *Modern Robotics: Mechanics, Planning, and Control.* Cambridge Univ. Press, 2017.

[22] F. C. Park, J. E. Bobrow, and S. R. Ploen, "A lie group formulation of robot dynamics," *Int. J. Robot. Res.*, vol. 14, no. 6, pp. 609–618, 1995.

[23] F. S. Grassia, "Practical parameterization of rotations using the exponential map," *J. Graph. Tools*, vol. 3, no. 3, pp. 29–48, 1998.

[24] O. Bohigas, M. Manubens, and L. Ros, "A complete method for workspace boundary determination on general structure manipulators," *IEEE Trans. Robot.*, vol. 28, no. 5, pp. 993–1006, 2012.

[25] Universal Robot, "UR5 Technical specifications," 2016. [Online]. Available: https://www.universal-robots.com/media/50588/ur5_en.pdf